

Magnetic properties of epitaxial Cr/Cr_{99.65}Ru_{0.35} heterostructures

A.R.E. Prinsloo¹, C.J. Sheppard¹, A.M. Venter², E.E. Fullerton³, B.S. Jacobs¹ and K. C. Rule⁴

¹Department of Physics, University of Johannesburg, PO Box 524, Auckland Park, 2006

²Research and Development Division, Necs Limited, P.O. Box 582, Pretoria 0001, South Africa

³Center for Magnetic Recording Research, University of California, San Diego, 9500 Gilman Dr., La Jolla, CA 92093-0401, USA

⁴Bragg Institute, ANSTO, Locked Bag 2001, Kirrawee DC NSW 2232, Australia

Author e-mail address: alettap@uj.ac.za

Abstract. We investigate the magnetic properties of these Cr/Cr_{99.65}Ru_{0.35} hetero-structures, with 10-nm Cr_{99.65}Ru_{0.35} layers and the Cr layer thickness fixed at 10 and 50 nm. Previous resistivity measurements probed the dimensionality effects in epitaxial and polycrystalline Cr_{100-x}Ru_x alloy thin films, as well as on epitaxial Cr/Cr_{99.65}Ru_{0.35} heterostructures. These results suggested proximity induced magnetism in the Cr layers with thickness less than 30 nm. In the present investigation the magnetic properties are directly studied through exploratory neutron diffraction measurements. The temperature dependence of the neutron results indicates the existence of the paramagnetic phase, as well as commensurate and incommensurate spin-density-wave phases in these hetero-structures. Present results therefore confirm key characteristics of the magnetic ordering in these layers.

1. Introduction

Bulk Cr is an itinerant electron antiferromagnetic material that forms an incommensurate (I) spin-density-wave (SDW) phase below its Néel temperature $T_N = 311$ K [1]. Cr and Cr alloys with their SDW antiferromagnetism, exhibit a richness of magnetic phenomena that has attracted considerable interest for many years [1].

Substantial focus has in recent years been placed on the investigation of magnetic properties in thin films and hetero-structures of Cr and Cr alloys, which have revealed fascinating properties not observed in bulk material [2, 3]. These properties include the mediating role of Cr thin films in exchange coupled super lattices and in giant magneto resistive (GMR) materials [4]. In order to broaden this knowledge, a previous contribution reported on dimensionality effects in epitaxial and polycrystalline Cr_{100-x}Ru_x alloy monolayer thin films, as well as on epitaxial Cr/Cr_{99.65}Ru_{0.35} hetero-structures [5]. The choice of this alloy system was based on the interesting behaviour seen in the bulk Cr_{100-x}Ru_x alloy system, where a commensurate (C) SDW phase is induced at a critical concentration $x_L \approx 0.2$ and temperature $T_L = 331$ K. Outstanding magnetic properties, such as exceptionally large concentration and pressure derivatives of T_N and peculiar magneto-elastic properties that have been studied extensively in CSDW Cr_{100-x}Ru_x bulk alloys and single crystals containing $x = 0.3$ [1].

Extending Cr-Ru alloy studies to include thin films and hetero-structures will explore the role of dimensionality and microstructure effects on the properties of this alloy system and further probe proximity effects in a purely itinerant magnetic system. Previous resistance studies [5] on Cr-Ru thin films and Cr/Cr_{99.65}Ru_{0.35} hetero-structures showed thought-provoking properties that also suggested proximity induced magnetism in the Cr layers with thickness less than 30 nm. In order to fully understand the behaviour of the SDW of Cr in these hetero-structure configurations, neutron diffraction studies on the Cr/Cr_{99.65}Ru_{0.35} hetero-structures are required, following the same approach as was previously used for Cr/Cr-Mn super lattices in which pinning and temperature hysteresis of the Cr SDW order with temperature was observed [2].

In this paper the results of exploratory neutron diffraction studies done on the Cr/Cr_{99.65}Ru_{0.35} hetero-structures are discussed and possible future measurements are proposed.

2. Experimental

Cr/Cr_{99.65}Ru_{0.35} hetero-structures were grown using DC magnetron sputtering onto MgO(100) substrates. A 10 nm Cr buffer layer was first deposited at 800°C, where after the hetero-structures were deposited at a lower temperature of 400°C to avoid inter-diffusion between the layers. The Cr_{99.65}Ru_{0.35} layers were co-sputtered from elemental sources maintaining a 10-nm layer thicknesses for both samples. For the two samples of this study the Cr inter-layer separation thicknesses (t_{Cr}) are fixed at 10 and 50 nm. All samples were prepared with a total thickness of approximately 700 nm. The concentrations and thicknesses of the various layers in the hetero-structures were confirmed using Rutherford Back Scattering (RBS) techniques, while the film crystallographic structure was characterized using X-ray diffraction (XRD) techniques. Magnetic phenomena were studied with electrical resistance (R) measurements, using standard DC four-probe methods, to determine the Néel transition temperatures (T_N). Magnetic properties were directly probed with neutron diffraction investigations on the Taipan triple-axis spectrometer at ANSTO (Australia) to determine the magnetic structure as a function of temperature. By utilizing the triple-axis instrument in elastic mode a very low background contribution could be attained, providing a sensitive probe notwithstanding the small volume of material available to scatter from and associated magnetic moments in the Cr/Cr_{99.65}Ru_{0.35} hetero-structures.

3. Results

Figure 1 shows the RBS spectrum for a [Cr(20 nm)/Cr-Ru(5 nm)]_{*n*} hetero-structure sample (black line), where the number of repeats $n = 8$. From this figure it is noted that the top four layers are better resolved than the bottom four layers. The simulated spectrum (red line) shows eight clear peaks, thus indicating that minimal diffusion of Ru occurred between the various layers. Further RBS spectra obtained with the sample tilted at different angles with reference to the beam reveals some roughness in the layers.

In figure 2 the XRD results are shown for the two different Cr/Cr_{99.65}Ru_{0.35} heterostructures. The results indicate that both the samples had epitaxial crystallite orientations with preferred growth directions [200]. The lattice parameter of the two structures rendered values of 0.28873 and 0.28869 nm for the $t_{Cr} = 10$ nm and $t_{Cr} = 50$ nm samples respectively. The full-width at half-maximum (FWHM) of the Bragg peaks was used to determine the length scale over which the films are structurally coherent (in growth direction) [6] by applying the Debye-Scherrer formula and neglecting instrumental resolution contributions. The crystal coherence lengths for both structures are similar, approximately 255 nm. The mosaic spread determined from the FWHM of rocking curves [6] were determined to be 0.55° and 0.61° respectively for $t_{Cr} = 10$ nm and 50 nm. Comparisons of in-plane and normal XRD scans indicate a normal plane strain of approximately 0.4%, that can be attributed to sample-substrate mismatch.

The Néel temperatures (T_N) of the films were determined from anomalies observed in electrical resistance (R) measurements as a function of temperature (T). The measured $R - T$ curves for the two Cr/Cr_{99.65}Ru_{0.35} hetero-structures are shown in figure 3 (a) and (b). Since only weak anomalies were

observed, T_N values were taken at the inflection point on the $R - T$ curves by considering the dR/dT versus T curves and taking T_N as the temperature of the minimum on each curve as shown in the insets of Figs 3 (a) and (b). The T_N values for the hetero-structures with t_{Cr} fixed at 10 nm and 50 nm were found to be 393 ± 4 K and 298 ± 3 K, respectively.

Previous research has shown that neutron diffraction investigations are well suited to determine the nature of the SDW ordering and to locate T_N in Cr and Cr alloys [7, 8, 9]. The presence of magnetic satellites at the $(1 \pm \delta, 0, 0)$ position confirms the presence of the incommensurate (I) SDW, while the absence of these satellites with only a central peak confirms that the sample is in the CSDW phase [1].

The neutron diffraction investigations on the hetero-structures were technically challenging in that the sample orientations had to be very specific with reference to the instrumental geometry to enable observation of the magnetic scattering from the Cr multilayers. The approach followed was to firstly orientate the MgO(100) single crystal substrates taking cognisance that the orientations of the magnetic coatings would be 45° rotated in the vertical plane due to the epitaxial orientation of Cr to MgO(100).

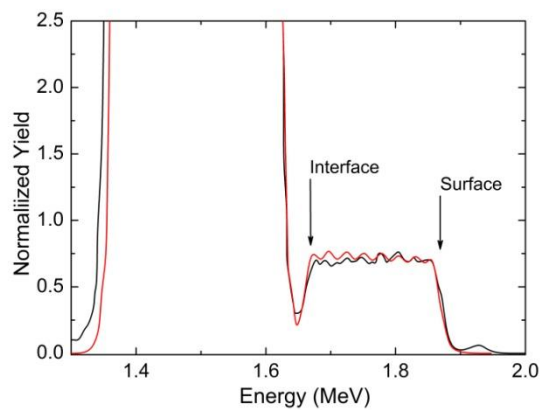


Figure 1: The RBS spectrum for a typical $[Cr/Cr-Ru]_n$ hetero-structure sample in which $n = 8$. The black line shows the measured spectrum for the sample and the red line the simulated spectrum.

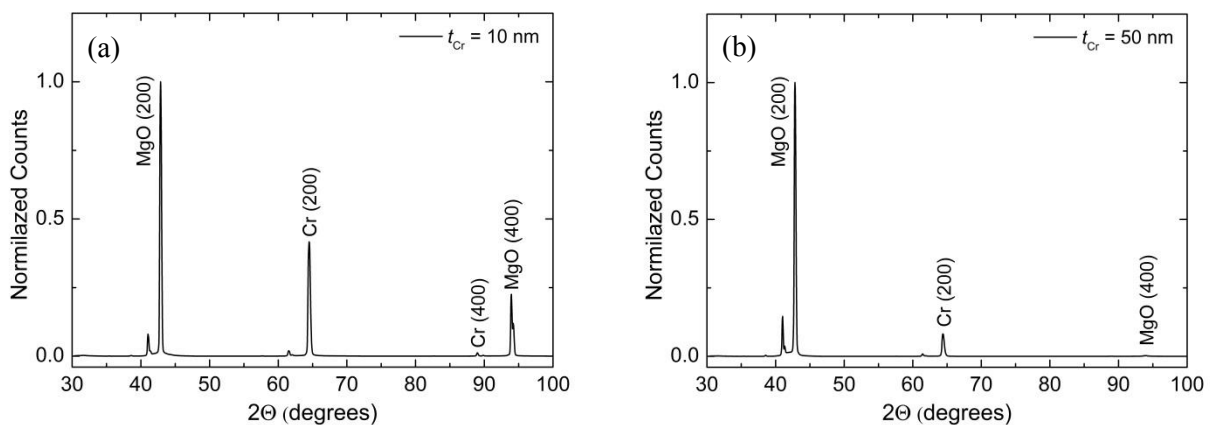


Figure 2: θ - 2θ XRD scans (Bragg-Brentano geometry) in which the scattering vector is maintained normal to the plane of the film, for the $Cr/Cr_{99.65}Ru_{0.35}$ hetero-structures prepared on MgO(100) substrates with t_{Cr} : (a) 10nm; and (b) 50 nm. The two unlabelled reflections at approximately 41° are possibly due to Cu K_β reflection of the MgO(200) peak.

The correlation geometries between the substrate and coating orientations are indicated in Fig. 4. Substrate reflections are indicated in black, Cr/Cr-Ru coating reflections in blue and the magnetic reflections in red. A correlation matrix that links the crystal and laboratory systems (UB matrix) was setup from the orientation optimised single crystal reflections. This was then used to explore the reflections of the Cr coating based on the corrected lattice parameter and crystalline reflections (020), (111) and (101) indicated in blue. After optimisation, the magnetic (001) reciprocal lattice position was explored in the reciprocal lattice direction q_{\parallel} , by performing (0, 0, z) scans, covering the range z range of 0.8 to 1.2 in steps of 0.002 in. The intensity at the (001) position would be purely of magnetic origin due to the structure factor of the bcc crystalline structure of the Cr/Cr-Ru. Taking cognisance that the coatings were typically 700 nm in thickness, prolonged data acquisition times had to be employed for good counting statistics to identify the diffraction signals.

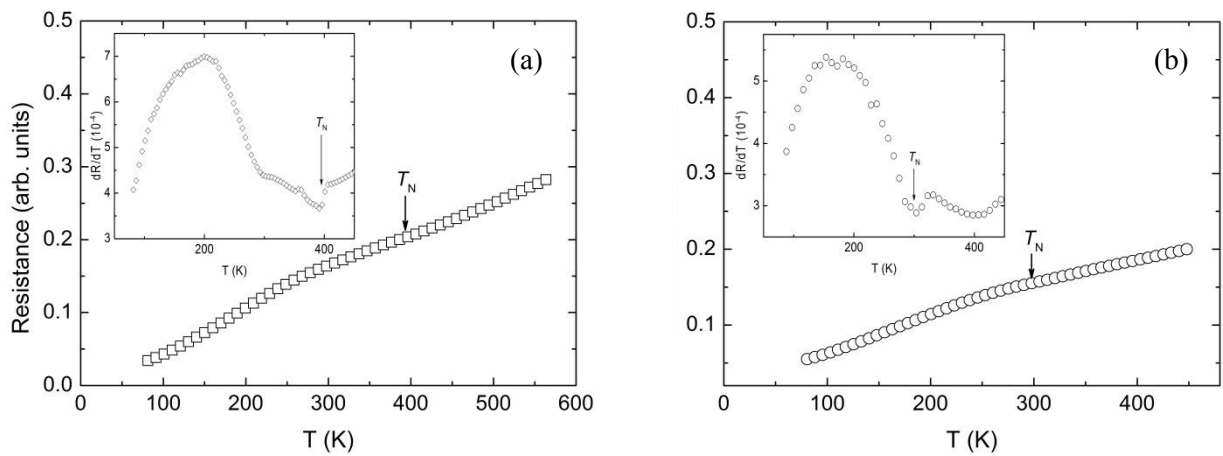


Figure 3: Resistance (R) versus temperature (T) graphs for Cr/Cr_{99.65}Ru_{0.35} hetero-structures prepared on MgO(100) substrates with t_{Cr} : (a) 10nm; and (b) 50 nm. The insets show dR/dT versus T for each sample with the temperature of the minimum taken as the Néel temperature (T_N).

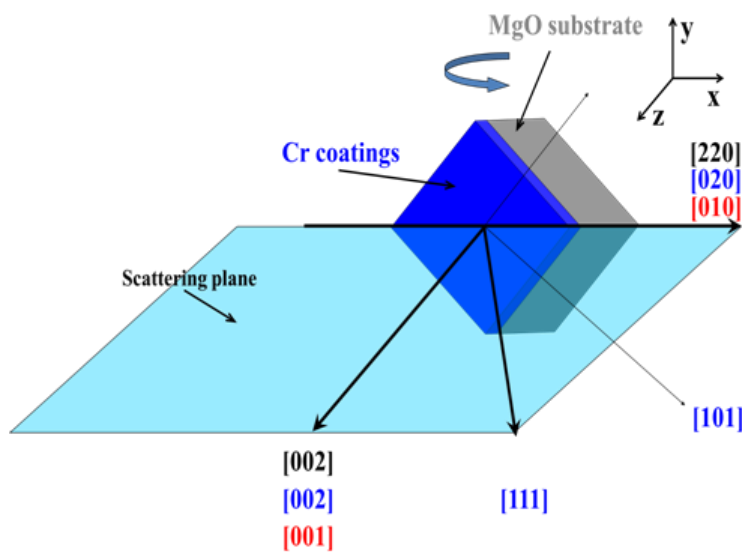


Figure 4: Sample orientation and expected reflections. Substrate reflections are indicated in black, Cr-Ru coating reflections in blue and the magnetic reflections in red.

Results from q_l reciprocal-lattice scans of the $(0,0,1-\delta)$ regions of the $\text{Cr}/\text{Cr}_{99.65}\text{Ru}_{0.35}$ hetero-structures prepared on $\text{MgO}(100)$ substrates with $t_{\text{Cr}} = 10$ nm and 50 nm are shown in Figs. 5 and 6, respectively. Reciprocal-lattice scans of the $t_{\text{Cr}} = 10$ nm hetero-structure were taken at constant T in the sequence 300 K, 200 K, 130 K and 450 K, i.e. respectively below and above the expected Néel temperature (from the resistance measurements expected to be just above room temperature) and to search for possible magnetic phase transformations below T_N . The scan at 450 K clearly demonstrates the absence of magnetic ordering, i.e. sample is in the paramagnetic state. The peak at $q_l \approx 0.92$ showed no temperature dependence and is assumed to originate from higher-order wavelength contamination from the $\text{MgO}(100)$ substrate that, notwithstanding $(2 \times 5\text{cm})$ PG beam filters employed, remained intense compared to the intensity of the magnetic peaks. For all the temperatures lower than 300 K diffraction peaks of magnetic origin are observed. The temperature dependences of q_l scans clearly revealed the presence of an ISDW phase below 200 K, and a CSDW phase at room temperature (300 K), with the Néel transition taking place between the room temperature 450 K measurements. A weak peak is observed at $q_l = 1.05$ in the 300 K data, but this is attributed the effect of a sloping background. It is thus concluded that a CSDW-ISDW phase transition takes place between 300 K and 200 K. The period of the ISDW phase does not seem to display temperature dependence. This may be expected if the SDW wavelength is constrained by the periodicity of the layers and therefore will not show any T dependence.

Results for the $\text{Cr}/\text{Cr}_{99.65}\text{Ru}_{0.35}$ hetero-structure with $t_{\text{Cr}} = 50$ nm, shown in Fig. 6, rendered much weaker magnetic ordering with the peaks of magnetic origin being only slightly higher than background, though the background being at least 5 times higher compared to the other sample. Conclusions drawn from the results are that the Néel transition occurs close to 300 K, since the magnetic ordering at 300 K is weakly commensurate, with an ISDW-to-CSDW phase transition taking place between 200 K and 300 K. In contrast to the sample with $t_{\text{Cr}} = 10$ nm the period of the ISDW phase seem to display a temperature dependence in this hetero-structure.

4. Conclusions

Exploratory neutron data resulting from this investigation support the conclusions made from resistance data, indicating that the T_N values for the hetero-structures with t_{Cr} fixed at 10 nm and 50 nm can be fixed at 393 ± 4 K and 298 ± 3 K, respectively. Most interesting, it is noted that from the neutron data it is evident that both samples show ISDW-CSDW phase transitions. These were not detected in resistivity measurements and needs to be investigated in more detail.

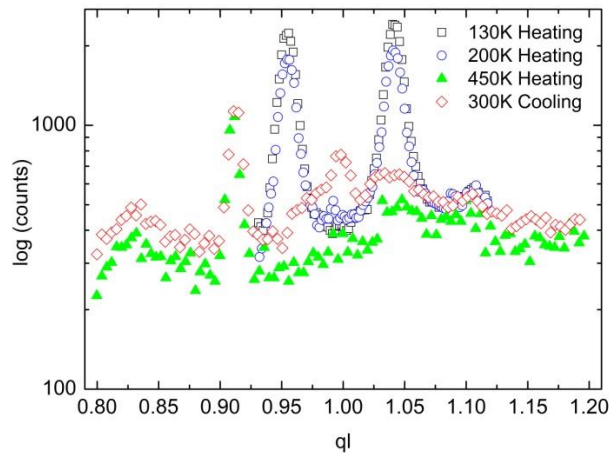


Figure 5: Reciprocal q_l lattice scans of the (100) position of sample $\text{Cr}/\text{Cr}_{99.65}\text{Ru}_{0.35}$ hetero-structure with $t_{\text{Cr}} = 10$ nm taken at various constant temperatures.

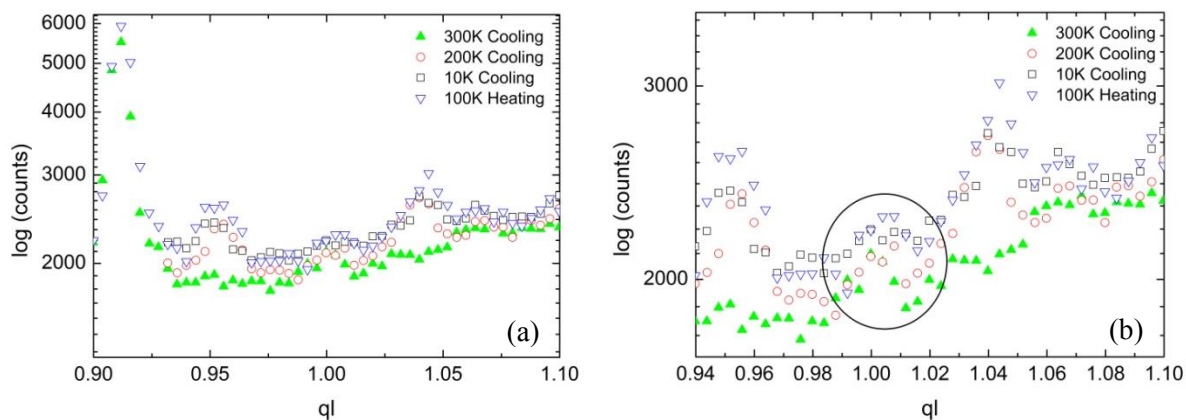


Figure 6: Reciprocal ql lattice scans of the (100) region in sample $\text{Cr}/\text{Cr}_{99.65}\text{Ru}_{0.35}$ hetero-structures with $t_{\text{Cr}} = 50$ nm taken at various constant temperatures. Figure (a) shows the wide ql range employed (searching for higher order resonance magnetic peaks), while figure (b) shows the region of the primary magnetic reflections close to the (100) position. The weak central peak indicative of the CSDW phase, is emphasized.

The present results indicate that it is feasibility to measure the magnetic ordering in Cr multilayer systems with the Taipan instrument at ANSTO and will pave the way for further studies on the sample series. Investigation of both samples warrant further research in order to better characterize the magnetic ordering by measurements at a number of additional temperatures. Furthermore, in considering the present results, it is clear that better data quality can be obtained by employing at least double the measurement times for sample with $t_{\text{Cr}} = 10$ nm, especially close to the Néel transition. At least four times longer data acquisition times is required for the sample with $t_{\text{Cr}} = 50$ nm, in conjunction with attempting to reduce the background. In addition special care needs to be taken to reduce the higher-order wavelength contamination of the beam, as well as improving the non-flat background.

Future neutron diffraction work on the $\text{Cr}/\text{Cr}_{99.65}\text{Ru}_{0.35}$ hetero-structures also needs to include scanning along other reciprocal lattice directions – specifically exploring the qk orientation. This should render results in line with that obtained for the $\text{Cr}/\text{Cr-Mn}$ system [2] in which pinning of the Cr SDW was observed and confirmed through neutron diffraction studies.

Acknowledgements

Financial support from the SA NRF (Grant Nos. 80928 and 80631) is acknowledged. ANSTO is acknowledged for the neutron diffraction beam time awarded.

References

- [1] Fawcett E., Alberts H.L., Galkin V. Yu, Noakes D.R., Yakhmi J.V. 1994 *Rev. Mod. Phys.* **66** 25
- [2] Fullerton E.E., Robertson J.L., Prinsloo A.E.R., Alberts H.L., Bader S.D. 2003 *Phys. Rev. Lett.* **91** 237201
- [3] Kumamuru R.K., Soh Y.A. 2008 *Nature* **452** 859
- [4] Zabel H.J. 1999 *J. Phys.: Condens. Matter* **11** 9303
- [5] Prinsloo A.E.R., Derrett H.A., Hellwig O., Fullerton E.E., Alberts H.L., van den Berg N. 2010 *J. Magn. Magn. Mat.* **322** 1126
- [6] Mattson J.E., Fullerton E.E., Sowers C.H., Bader S.D. 1995 *J. Vac. Sci. Technol. A* **13**(2) 276
- [7] Baran A., Alberts H.L., Strydom A.M. and du Plessis P. de V. 1992 *Phys. Rev.* **B 45** 10473
- [8] Bacon G.E. 1961 *Acta. Cryst.* **14** 823
- [9] Koehler W.C., Moon R.M., Trego A.L. and Mackintosh A.R. 1966 *Phys. Rev.* **151** 405